

# Investigation of the $\text{TiCl}_4$ Reaction Order in Living Isobutylene Polymerizations

J. E. Puskas\* and M. G. Lanzendörfer

Department of Chemical and Biochemical Engineering, University of Western Ontario,  
London Ontario, Canada N6A 5B9

Received June 12, 1998; Revised Manuscript Received September 24, 1998

**ABSTRACT:** The reaction order with respect to  $\text{TiCl}_4$  was investigated in the living polymerization of isobutylene (IB) initiated by 2-chloro-2,4,4-trimethylpentane (TMPCl)/ $\text{TiCl}_4$  in hexane/methyl chloride (Hx/MeCl) 60/40 v/v cosolvents at  $-80^\circ\text{C}$ . It was found that the reaction is more complex than previously believed. The  $\text{TiCl}_4$  order was found to be closer to 1 at  $[\text{TMPCl}]_0 > [\text{TiCl}_4]_0$ , and closer to 2 when  $[\text{TMPCl}]_0 < [\text{TiCl}_4]_0$ . Kinetic complexity is demonstrated by the fraction order in  $\text{TiCl}_4$ , and the rate-acceleration found when  $[\text{TMPCl}]_0 \gg [\text{TiCl}_4]_0$ . A comprehensive mechanistic scheme to explain the kinetic behavior of living IB polymerizations is proposed. Further, a new fiber optic mid-IR monitoring method for more convenient kinetic investigations is demonstrated.

## Introduction

The kinetics and mechanism of the controlled/living polymerization of isobutylene (IB) have been the subject of intense investigations.<sup>1–15</sup> It is now generally accepted that in living IB polymerizations co-initiated by Lewis acids such as  $\text{TiCl}_4$  and/or  $\text{BCl}_3$ , the chlorine-terminated inactive chain ends are in dynamic equilibrium with a very small concentration of active ionic species, as first suggested by Kaszas et al.<sup>11</sup> The active ionic species were suggested to be ion pairs,<sup>16</sup> and this suggestion was corroborated by the kinetic investigations of Storey et al.<sup>7</sup> While the various systems investigated differ in the nature of initiator (I), additives (electron pair donor (ED) or proton trap), and solvents, the kinetic order with respect to initiator has been reported to be invariably 1. The reaction order in monomer was found to be 1 in most cases, but apparent zero order monomer dependence has also been reported.<sup>9,12–14</sup> The reaction order with respect to the Lewis acid  $\text{TiCl}_4$  has been unclear and was the focus of this investigation. Most research groups reported a second-order dependency on  $\text{TiCl}_4$  concentration, but Kaszas et al.<sup>4</sup> and Kennedy et al.<sup>15</sup> claimed first-order dependence under certain conditions. Kaszas et al. obtained first-order dependence in MeCHx/MeCl cosolvents under conditions where  $[\text{TiCl}_4]_0 \leq [\text{I}]_0$ , while second-order dependency was invariably obtained in Hx/MeCl or Hx/MeCl<sub>2</sub> cosolvents under conditions where  $[\text{TiCl}_4]_0 > [\text{I}]_0$ , with one exception.<sup>15</sup> Independent investigations revealed the tendency of  $\text{TiCl}_4$  to form dimers only at cryogenic temperatures (12 K)<sup>17</sup> and/or at high concentration (25 mol %  $\text{TiCl}_4$  in  $\text{CCl}_4$  at 300 K).<sup>18</sup> In the living block copolymerization of IB with isobutyl vinyl ether (IBVE) initiated by TMPCl/ $\text{TiCl}_4$  in Hx/MeCl 60/40 (v/v) solvent mixture at  $-90^\circ\text{C}$ , blocking was facilitated by capping the living PIB chain end with diphenylethylene (DPE) prior to the addition of IBVE. Under conditions when  $[\text{LA}]_0 \leq 2[\text{chain end}]$ , incomplete ionization of DPE-capped chain ends was found. This was explained by the coexistence of monomeric and dimeric counterions.<sup>19</sup> In a recent NMR study of the ionization equilibria of cumyl chloride in  $\text{CD}_2\text{Cl}_2$  between  $-50$  and  $-90^\circ\text{C}$ , the equilibrium constant was found to have a very strong temperature dependence.

With  $[\text{TiCl}_4]_0/[\text{I}]_0 = 0.9$ , about 10% of the initiator was ionized at  $-60^\circ\text{C}$ , while the extent of ionization was nearly 70% at  $-90^\circ\text{C}$ . However, complete ionization was not achieved even at a ratio of  $[\text{TiCl}_4]_0/[\text{I}]_0 = 2$ . This was explained by the formation of dimeric counteranions in a consecutive reaction scheme through a monomeric stage.<sup>20</sup> In addition, Storey and Choate showed that in living IB polymerization second-order dependence involving dimeric  $\text{Ti}_2\text{Cl}_9^-$  counteranions can be explained only by reaction of additional  $\text{TiCl}_4$  with monomeric counteranions, not by direct ionization of chains by neutral dimeric  $\text{Ti}_2\text{Cl}_8$ .<sup>7</sup>

While continued studies provide information regarding living IB polymerization, there is no comprehensive kinetic/mechanistic model available today. In an attempt to develop a comprehensive model, we decided to systematically investigate the kinetics of this reaction. The study of the  $\text{TiCl}_4$  reaction order and a comprehensive mechanistic model are reported. A new fiber optic mid-IR monitoring technique developed for more convenient kinetic studies is demonstrated.

## Experimental Section

**Materials.** Titanium tetrachloride ( $\text{TiCl}_4$ ), and di-*tert*-butylpyridine (DtBP) were used as received (Aldrich). Hexane (Hx) and methylcyclohexane (MeCHx) (Caledon) were freshly distilled from  $\text{CaH}_2$  prior to use. 2,4,4-Trimethyl-2-chloropentane (TMPCl) was synthesized as described.<sup>21</sup> It was purified by distillation, and purity was determined by  $^1\text{H}$  NMR. Methyl chloride (MeCl) and isobutylene (IB) were dried by passing the gases through drying columns packed with  $\text{CaCl}_2/\text{BaO}$ .

**Procedures. Polymerizations.** Polymerizations were carried out in an Mbraun LabMaster 130 glovebox under dry nitrogen at  $-80^\circ\text{C}$ . The moisture ( $<1$  ppm) and oxygen (5 ppm) content were monitored. The hexane bath was cooled with an FTS Flexi Cool Immersion Cooler. A 500 mL round-bottom flask equipped with overhead stirrer was charged with MeCl and Hx (40/60 v/v) or MeCl and MeCHx (40/60 v/v). TMPCl was added to the mixture, followed by the addition of DtBP and IB (concentrations are specified in the text or figure captions). Appropriate amounts of IB and MeCl were condensed into prechilled graduated cylinders before addition to the reactor. The reaction was started by the addition of a chilled stock solution of  $\text{TiCl}_4$  in Hx or MeCHx. Samples were taken at specified times into chilled culture tubes containing methanol for gravimetric conversion analysis. A reaction was

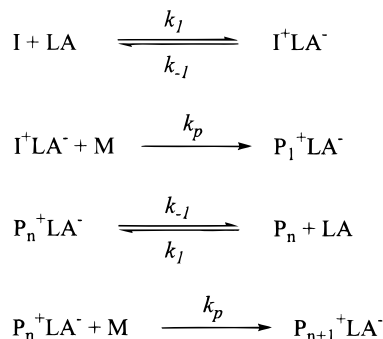
also followed by the simultaneous direct monitoring of IB consumption and PIB formation by a fiber optic immersion attenuated total reflection (ATR) IR probe (Remspec) attached to a BioRad FTIR instrument, using BioRad WinIR software. Reactions were terminated at specified times by addition of prechilled methanol to the charge. Solvents were evaporated, and the polymers were purified by redissolving them in Hx, washing with distilled water, drying over MgSO<sub>4</sub>, filtering and precipitating from methanol, and drying in a vacuum oven. Conversions were determined by gravimetry or by the ratio of the relevant IR band intensities at time zero and the sampling time.

**Polymer Analysis.** Polymer molecular weights (MW) and molecular weight distributions (MWD) were determined by size exclusion chromatography (SEC) using a Waters system equipped with six Styragel-HR columns (100, 500, 10<sup>3</sup>, 10<sup>4</sup>, 10<sup>5</sup>, and 10<sup>6</sup> Å pore sizes), thermostated to 35 °C, a Waters 410 DRI detector thermostated to 40 °C, and a Waters 996 PDA detector set at 254 nm. THF, freshly distilled from CaH<sub>2</sub>, was employed as the mobile phase and was delivered at 1 mL/min. MWs were calculated by using the Universal Calibration Principle, which was shown to be valid for linear PIBs.<sup>22</sup>

## Results and Discussion

In our kinetic investigations we elected to use the system suggested by Kaszas et al.<sup>4</sup> The initiator used was TMPCl, a model compound for PIB chain ends. The use of TMPCl was suggested for kinetic investigations because it was assumed that  $k_i = k_p$ , and the initiator–TiCl<sub>4</sub> (I–LA) equilibrium is the same as the polymer–TiCl<sub>4</sub> (P<sub>n</sub>–LA) equilibrium (Scheme 1). However, Mayr

**Scheme 1. I–LA and P<sub>n</sub>–LA Equilibria**



et al.<sup>14</sup> used both TMPCl and the trimer chloride of IB as initiators for IB polymerizations and found the trimer chloride to be a better model for the growing PIB chain. Because we wanted to compare our results to past work, TMPCl was selected as initiator for this study. Since the role of EDs in living IB polymerizations is still debated, no ED was used in our kinetic experiments. While EDs were demonstrated to be instrumental in block copolymerizations,<sup>23</sup> living IB polymerizations were achieved using only DtBP as a proton trap. Faust suggested that the sole role of strongly complexing EDs is scavenging protic impurities.<sup>1</sup> However, as Storey pointed out, this simplified theory fails to account for experimentally observed effects of various complexing EDs on polymerization rates and molecular weight distributions.<sup>7</sup> It is possible that strongly complexing EDs play a dual role of proton scavenging and interacting with the active centers. The nature of this interaction is not clear—it may be that the EDs affect the ionization equilibrium and/or stabilize the carbocations. Further research is needed to clarify the role of EDs. To avoid protic initiation, we used DtBP, which is suggested to be exclusively a proton trap.<sup>5</sup> In our

kinetic investigations regarding the TiCl<sub>4</sub> order, polymerizations were carried out at both  $[\text{LA}]_0 \leq [\text{I}]_0$  and  $[\text{LA}]_0 > [\text{I}]_0$ . In each set of experiments only the TiCl<sub>4</sub> concentration was varied while the concentration of all the other compounds (initiator, DtBP, IB) was kept constant.

$[\text{LA}]_0 \leq [\text{I}]_0$ . This most interesting concentration range has only been investigated by Kaszas et al.<sup>4</sup> for TiCl<sub>4</sub> and Mayr et al.<sup>14</sup> for BCl<sub>3</sub>. Interestingly, initiation and propagation proceed simultaneously and both monomer and initiator consumption can be followed (initiator consumption data are derived from molecular weight and monomer conversion data). Kaszas et al.<sup>4</sup> developed the following rate equations:

$$\ln \frac{[\text{I}]_0}{[\text{I}]} = k_1 [\text{LA}]_0 t \quad (1)$$

$$\ln \frac{[\text{M}]_0}{[\text{M}]} = k_p' [\text{I}]_0 [\text{LA}]_0 t \quad (2)$$

where  $k_p' = k_p K_1 = k_p k_1 / k_{-1}$ . It was shown that under the conditions reported (TMPCl initiator, TiCl<sub>4</sub> co-initiator, DtBP proton trap, MeCl/MeCHx 40/60 v/v solvent mixture, –90 °C) and at  $[\text{LA}]_0 \leq [\text{I}]_0$ , both the initiation and propagation were first order in  $[\text{TiCl}_4]$ , and  $k_p' = 0.33 \text{ L}^2/\text{mol}^2 \text{ s}$ ,  $k_1 = 0.02 \text{ L/mol s}$ , and  $k_p/k_{-1} = 16.5$  were reported. The constancy of  $k_p'$  with varying  $[\text{TiCl}_4]$  was used to demonstrate first-order TiCl<sub>4</sub> dependence for propagation. Using the rate constant of propagation for cationic IB polymerization ( $k_p = 6 \times 10^8 \text{ L/mol s}$ ) measured recently by Roth and Mayr,<sup>24</sup> from eq 2 we get  $K_1 = 5.5 \times 10^{-10}$  and  $k_{-1} = 3.6 \times 10^7 \text{ L/mol s}$ . We repeated the experiments of Kaszas et al.<sup>4</sup> at –80 °C and, in agreement with the reported results, found first-order dependence in TiCl<sub>4</sub> for both initiation and propagation with constant  $k_p'$  and  $k_1$ . Figures 1 and 2 show the results;  $k_p' = 0.55$  and  $0.53 \text{ L}^2/\text{mol}^2 \text{ s}$ , and  $k_1 = 0.024$  and  $0.025 \text{ L/mol s}$  for  $[\text{LA}]_0 = [\text{I}]_0$  and  $[\text{LA}]_0 = 1/4 [\text{I}]_0$ , respectively. It should be emphasized that under conditions where  $[\text{LA}]_0 \leq [\text{I}]_0$ ,  $[\text{I}]$  and  $[\text{P}_n]$  are simultaneously changing, but the rate of polymerization remains constant. During this period  $[\text{I}] + [\text{P}_n] = [\text{I}]_0$ ; when all initiator is consumed,  $[\text{P}_n] = [\text{I}]_0$  and the constancy of polymerization rate becomes evident. This phenomenon is due to the fact that the rate is directly proportional to the active site concentration, for which a steady-state concentration can be considered. Similar phenomena were reported by Kamigaito et al.<sup>25</sup> for certain living vinyl ether polymerizations.

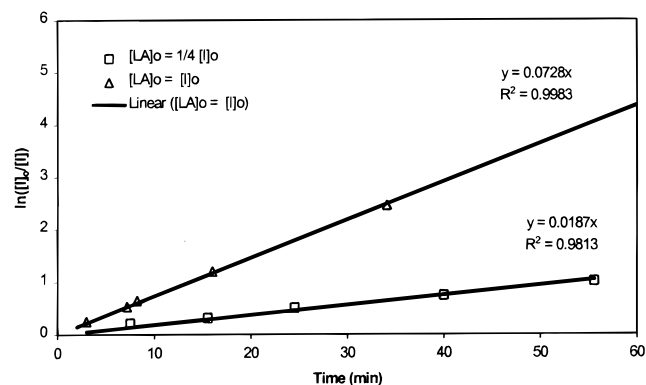


**Figure 1.**  $\ln([\text{I}]_0/[\text{I}])$  vs time plot for  $[\text{LA}]_0 \leq [\text{I}]_0$  in TMPCl/TiCl<sub>4</sub>-initiated IB polymerization at –80 °C.  $[\text{IB}]_0 = 2.0 \text{ M}$ ;  $[\text{DtBP}] = 7.0 \times 10^{-3} \text{ M}$ ;  $[\text{TMPCl}]_0 = 5.0 \times 10^{-2} \text{ M}$ ; MeCHx/MeCl = 60/40 (v/v).

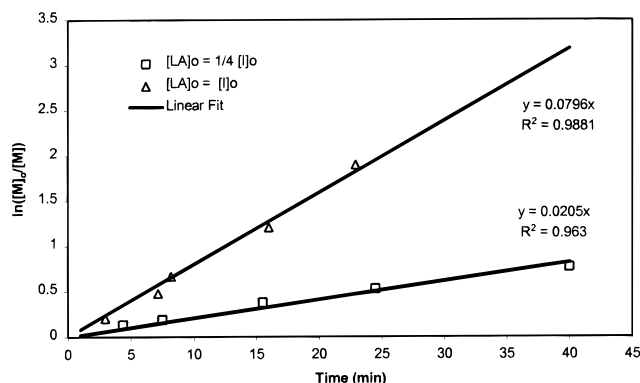


**Figure 2.**  $\ln([M]_0/[M])$  vs time plot for  $[LA]_0 \leq [I]_0$  in TMPCl/TiCl<sub>4</sub>-initiated IB polymerization at  $-80$  °C.  $[IB]_0 = 2.0$  M;  $[DTBP] = 7.0 \times 10^{-3}$  M;  $[TMPCl]_0 = 5.0 \times 10^{-2}$  M; MeCHx/MeCl = 60/40 (v/v).

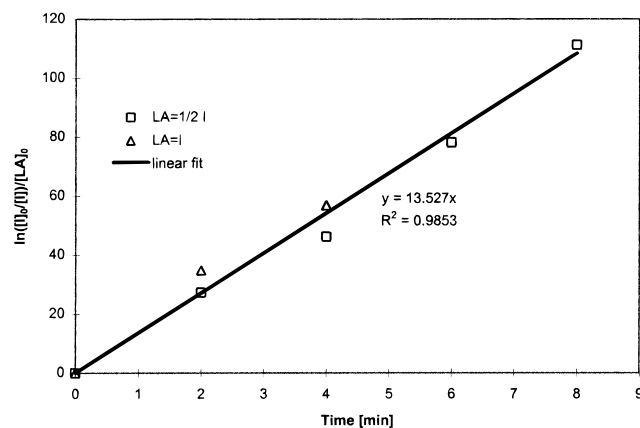


**Figure 3.**  $\ln([I]_0/[I])/[LA]_0$  vs time plot for  $[LA]_0 \leq [I]_0$  in TMPCl/TiCl<sub>4</sub>-initiated IB polymerization at  $-80$  °C.  $[IB]_0 = 2.0$  M;  $[DTBP] = 7.0 \times 10^{-3}$  M;  $[TMPCl]_0 = 5.0 \times 10^{-2}$  M; Hx/MeCl = 60/40 (v/v).

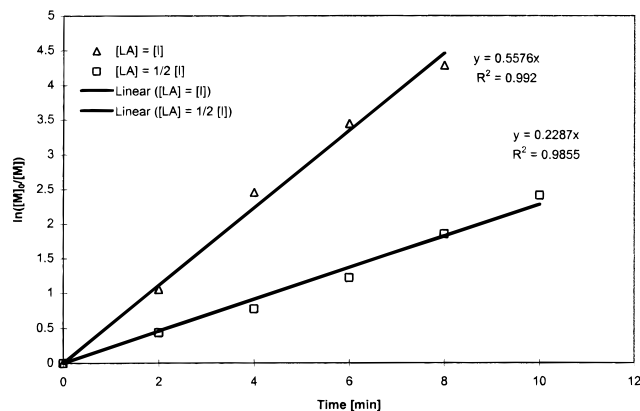


**Figure 4.**  $\ln([M]_0/[M])$  vs time plot for  $[LA]_0 \leq [I]_0$  in TMPCl/TiCl<sub>4</sub>-initiated IB polymerization at  $-80$  °C.  $[IB]_0 = 2.0$  M;  $[DTBP] = 7.0 \times 10^{-3}$  M;  $[TMPCl]_0 = 5.0 \times 10^{-2}$  M; Hx/MeCl = 60/40 (v/v).

Having established the reproducibility of the experiments reported by Kaszas et al.<sup>4</sup> we proceeded to conduct our studies using Hx as the nonpolar component of the solvent mixture. Comparison of our data obtained using Hx as the nonpolar cosolvent to those found using MeCHx revealed differences in rate constants. Figures 3 and 4 show first-order plots for initiation and propagation. Figure 3 yields  $k_1 = 0.22$  L/mol s, and Figure 4 yields  $k_p' = 3.7$  and  $3.1$  L<sup>2</sup>/mol<sup>2</sup> s for  $[LA]_0 = [I]_0$  and  $[LA]_0 = 1/2[I]_0$ , respectively. The small variation of  $k_p'$

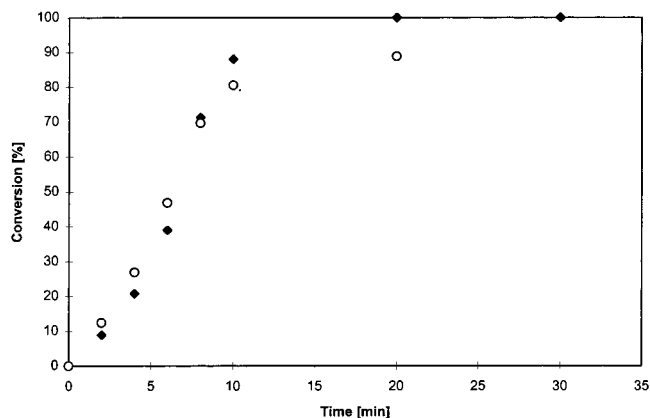


**Figure 5.** Conversion vs time plot for both initiator (○) and monomer (◆) for  $[LA]_0 = 1/4[I]_0$  in TMPCl/TiCl<sub>4</sub>-initiated IB polymerization at  $-80$  °C.  $[IB]_0 = 2.0$  M;  $[DTBP] = 7.0 \times 10^{-3}$  M;  $[TMPCl]_0 = 5.0 \times 10^{-2}$  M; Hx/MeCl = 60/40 (v/v).

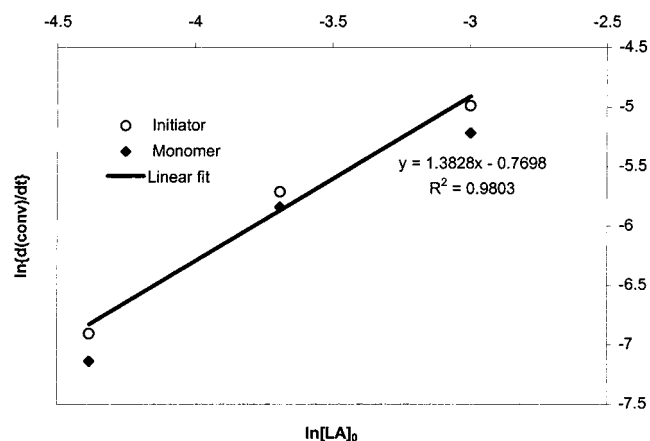


**Figure 6.** Linearized initial rate ( $\ln\{d(\text{conversion})/dt\}_{\text{initial}} \approx \ln\{\Delta(\text{conversion})/\Delta\text{time}\}$  at 2 min) vs  $\ln[LA]_0$  plots for both initiator (○) and monomer (◆) in TMPCl/TiCl<sub>4</sub>-initiated IB polymerization at  $-80$  °C.  $[IB]_0 = 2.0$  M;  $[DTBP] = 7.0 \times 10^{-3}$  M;  $[TMPCl]_0 = 5.0 \times 10^{-2}$  M; Hx/MeCl = 60/40 (v/v).

indicates nearly first-order dependence. Using an average of  $k_p' = 3.4$  L<sup>2</sup>/mol<sup>2</sup> s and  $k_p = 6 \times 10^8$  L<sup>2</sup>/mol<sup>2</sup> s,  $K_1$  was calculated from eq 2 to be  $K_1 = 5.6 \times 10^{-9}$ , and  $k_{-1} = 3.9 \times 10^7$  L/mol s. Surprisingly,  $K_1$  is 1 order of magnitude higher than that obtained in MeCl/MeCHx cosolvents. Again, while  $[I]$  and  $[P_n]$  are simultaneously changing, the polymerization rate remains constant. Interestingly, both the monomer and initiator conversion plots (Figure 5) show rate acceleration for  $[LA]_0 = 1/4[I]_0$ , demonstrating further complexity of the reaction. The nearly identical conversion profiles for initiator and monomer demonstrate that indeed  $k_i = k_p$ , and TMPCl is a good model for PIB chain ends. The S-shaped curves indicate consecutive reactions, perhaps a preequilibrium—this will be discussed in detail and incorporated into the comprehensive scheme. In the case of complex reactions, the order should be established by using the initial rate method. Figure 6 shows the normalized initial rate plots ( $\ln\{d(\text{conversion})/dt\}_{\text{initial}} \approx \ln\{\Delta(\text{conversion})/\Delta\text{time}\}$  at 2 min, vs  $\ln[LA]_0$ ) for initiation and propagation. The slope of the line yields an order of 1.38. Thus the reaction order with respect to TiCl<sub>4</sub> using Hx as a nonpolar cosolvent is higher than 1, and the rates of initiation and propagation are considerably faster than that obtained in MeCHx ( $k_p' \approx 3.4$  vs  $0.54$  L/mol s, respectively) at  $[LA]_0 < [I]_0$ .



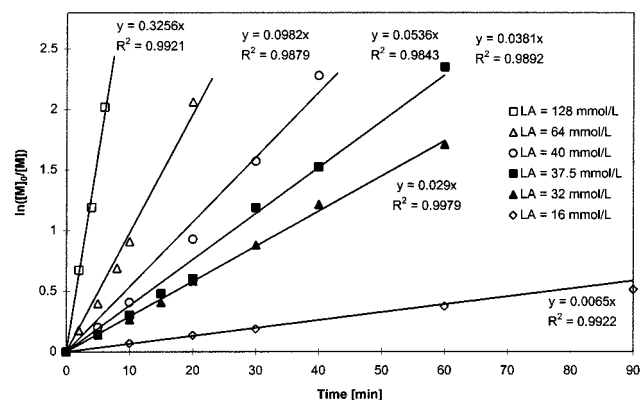


**Figure 7.**  $\ln[M]_0/[M]$  vs time plots for  $[LA]_0 > [I]_0$  in TMPCl/TiCl<sub>4</sub>-initiated IB polymerization at  $-80^\circ\text{C}$ .  $[IB]_0 = 2.0\text{ M}$ ;  $[DTBP] = 7.0 \times 10^{-3}\text{ M}$ ;  $[TMPCl]_0 = 4.0 \times 10^{-3}\text{ M}$ ; Hx/MeCl = 60/40 (v/v).

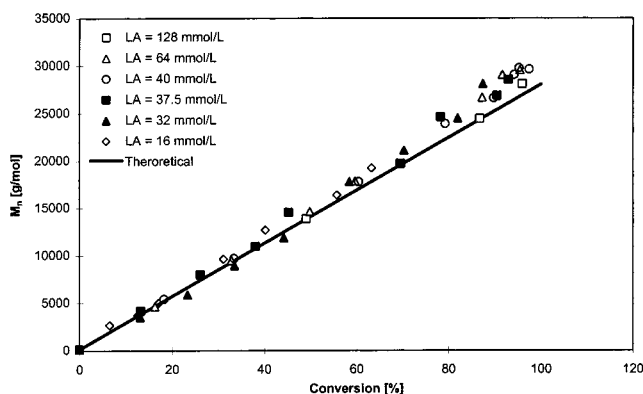


**Figure 8.**  $M_n$  vs conversion plot for  $[LA]_0 > [I]_0$  in TMPCl/TiCl<sub>4</sub>-initiated IB polymerization at  $-80^\circ\text{C}$ .  $[IB]_0 = 2.0\text{ M}$ ;  $[DTBP] = 7.0 \times 10^{-3}\text{ M}$ ;  $[TMPCl]_0 = 4.0 \times 10^{-3}\text{ M}$ ; Hx/MeCl = 60/40 (v/v).

**$[LA]_0 > [I]_0$ .** Experiments were conducted with varying Lewis acid concentrations greater than the initiator concentration. First-order plots of monomer consumption are shown in Figure 7. At  $[LA]_0 > [I]_0$ , initiation was instantaneous; therefore, initiator consumption could not be monitored. The  $M_n$  vs conversion plots were linear, as shown in Figure 8 and in very good agreement with theoretical values. The MWD decreased with conversion, reaching MWD = 1.2 in the final samples. Collectively, Figures 7 and 8 demonstrate living polymerization, i.e., no chain transfer and no irreversible termination. The  $\ln(d[M]/dt)$  vs  $\ln[LA]_0$  plot (Figure 9) shows that under these conditions the order of the reaction relative to  $[TiCl_4]$  is 1.76. This is in good agreement with values of 1.7–2.2 reported previously by other authors.<sup>5–7</sup> As mentioned earlier, TiCl<sub>4</sub> can dimerize and the dimer is a much stronger Lewis acid than the monomeric one; the relatively weak chloride acceptor  $Ti_2Cl_9^-$  ion thus formed has been characterized.<sup>26,27</sup>  $k_p' = \text{slope}/[I]_0[TiCl_4]_0$  and  $k_p^\wedge = \text{slope}/[I]_0[TiCl_4]_0^{1.76}$  values were calculated from Figure 7 and listed in Table 1. The  $k_p^\wedge$  values are constant within experimental error ( $k_p^\wedge(\text{average}) = 51.5\text{ L}^3/\text{mol}^3\text{ s}$ ) and independent of  $[TiCl_4]$ . The original simple model can then be rewritten as follows:

$$\ln \frac{[M]_0}{[M]} = k_p^\wedge [I]_0 [TiCl_4]^{1.76} t \quad (3)$$

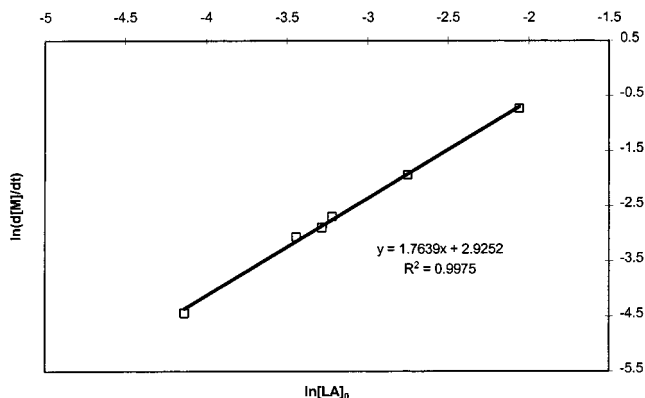


**Figure 9.**  $\ln(d[M]/dt)$  vs  $\ln[LA]_0$  plot for  $[LA]_0 > [I]_0$  in TMPCl/TiCl<sub>4</sub>-initiated IB polymerization at  $-80^\circ\text{C}$ .  $[IB]_0 = 2.0\text{ M}$ ;  $[DTBP] = 7.0 \times 10^{-3}\text{ M}$ ;  $[TMPCl]_0 = 4.0 \times 10^{-3}\text{ M}$ ; Hx/MeCl = 60/40 (v/v).

**Table 1.**  $k_p'$  and  $k_p^\wedge \sim k_p'' = K_0 K_2 k_p$  Values for  $[LA]_0 > [I]_0$  in TMPCl/TiCl<sub>4</sub>-Initiated IB Polymerization at  $-80^\circ\text{C}$  (See Also Figure 7)

$[TiCl_4]$ (mmol/L)	$k_p'$ ( $\text{L}^2/\text{mol}^2\text{ s}$ )	$k_p^\wedge$ ( $\text{L}/\text{mol s}$ )
16	1.7	50
32	3.8	52
37.5	4.2	50
40	5.6	54
64	6.4	52
128	10.6	51

$k_p^\wedge$  is a composite rate constant and the product of the rate constant of propagation  $k_p$  and one or more equilibrium constants.

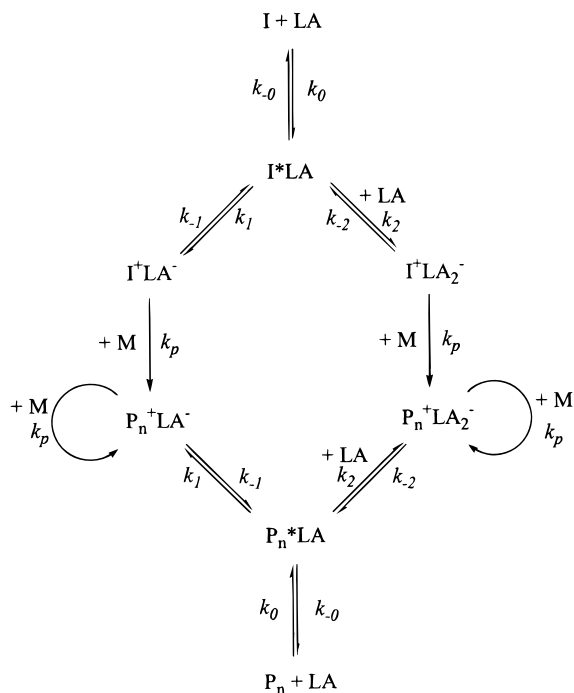
In kinetic studies published in the literature often the  $[I]_0/[TiCl_4]_0$  ratio is kept constant and the concentration of the whole initiating system is varied. For instance, in the latest paper of the Storey group  $[TiCl_4]_0 = 20[I]_0$  was used, and the  $\ln k_{app}$  vs  $\ln[\text{initiating system}]$  plot yielded slopes of about 3 at all temperatures investigated.<sup>7</sup> Substituting  $[LA]_0 = 20[I]_0$  into eq 3 readily yields the nearly third-order dependence, as shown in eq 4:

$$\ln \frac{[M]_0}{[M]} = K' [I]_0^{2.76} t \quad (4)$$

Data interpretation is greatly simplified when equations containing true constants such as eq 3 are used, and all the concentrations (which should be treated as independent variables) are separated. This approach is followed in our laboratory.

**Proposed Comprehensive Kinetic/Mechanistic Model of Living IB Polymerizations.** Our experimental results verified that at  $[LA]_0 \leq [I]_0$  living IB polymerizations are closer to first order in  $[TiCl_4]$ , while at  $[LA]_0 > [I]_0$  closer to second order was observed. The rate acceleration at  $[LA]_0 = 1/4[I]_0$  indicated a complex reaction even at  $[LA]_0 \leq [I]_0$ . On the basis of these results, and recent results concerning  $Ti_2Cl_9^-$  counteranion formation,<sup>7,20</sup> we propose a comprehensive mechanistic model for living IB polymerizations (Scheme 2).

This comprehensive scheme accounts for the existence of both monomeric and dimeric counteranions; further, the two-step formation of dimeric counteranions<sup>7,20</sup> is accounted for. We propose that at  $[LA]_0 \leq [I]_0$  the left side of the scheme dominates, due to a "shortage" of

**Scheme 2. Comprehensive Scheme for Living IB Polymerizations**

$\text{TiCl}_4$ , while at  $[\text{LA}]_0 > [\text{I}]_0$  the right side dominates. With this, eqs 1 and 2 should be modified as follows:

1.  $[\text{LA}]_0 \leq [\text{I}]_0$

$$\ln \frac{[\text{I}]_0}{[\text{I}]} = K_0 k_1 [\text{LA}]_0 t \quad (5)$$

$$\ln \frac{[\text{M}]_0}{[\text{M}]} = k_p' [\text{I}]_0 [\text{LA}]_0 t \quad (6)$$

where  $k_p' = K_0 k_p K_1 = K_0 k_p k_1 / k_{-1}$ .

2.  $[\text{LA}]_0 \gg [\text{I}]_0$

$$\ln \frac{[\text{I}]_0}{[\text{I}]} = K_0 k_2 [\text{LA}]_0^2 t \quad (7)$$

$$\ln \frac{[\text{M}]_0}{[\text{M}]} = k_p'' [\text{I}]_0 [\text{LA}]_0^2 t \quad (8)$$

where  $k_p'' = K_0 k_p K_2 = K_0 k_p k_2 / k_{-2}$ .  $K_0 k_1$  and  $K_0 K_1 k_p$  values can be obtained from first-order initiator and monomer consumption plots at  $[\text{LA}]_0 \leq [\text{I}]_0$ . Experimental evidence shown here suggests that when MeCHx is used as the nonpolar component of the solvent mixture, the first-order composite rate constant  $k_p'$  is considerably smaller compared to that measured with Hx as the nonpolar component. From Figures 1 and 2 we get  $K_0 k_1 = 0.0245 \text{ L/mol s}$  and  $K_0 K_1 k_p = 0.54 \text{ L}^2/\text{mol}^2 \text{ s}$ , as opposed to  $K_0 k_1 = 0.22 \text{ L/mol s}$  and  $K_0 K_1 k_p = 3.4 \text{ L}^2/\text{mol}^2 \text{ s}$  from Figures 3 and 4. These numbers yield  $k_{-1} = 3.1 \times 10^7 \text{ L/mol s}$  for MeCHx and  $k_{-1} = 3.9 \times 10^7 \text{ L/mol s}$  for Hx.  $k_p'' = K_0 K_2 k_p \approx k_p^\wedge$  values can be found from monomer consumption plots at  $[\text{LA}]_0 > [\text{I}]_0$ . Interestingly, no difference was found between the second-order rate constants measured in MeCHx and Hx. From Table 1,  $k_p^\wedge \approx k_p'' = K_0 K_2 k_p = 51.5 \text{ L}^3/\text{mol}^3 \text{ s}$  (average). The individual values for  $K_0$ ,  $K_1$ , and  $K_2$  cannot be deconvoluted from polymerization experi-

ments. However, under conditions of practical significance (i.e., at  $[\text{LA}]_0 \gg [\text{I}]_0$ ), the modified simple model shown in eq 3 can be used to predict monomer conversion, once  $k_p^\wedge$  is obtained from experimental data. Also, both  $k_p'$  and  $k_p^\wedge \approx k_p''$  contain equilibrium constants  $K_1$ ,  $K_0$ , and  $K_2$ , respectively, and hence, should be dependent on solvent composition, as shown by Mayr et al.<sup>14</sup> Since IB and PIB also serve as nonpolar components in the polymerization charge,  $k_p'$  and  $k_p^\wedge \approx k_p''$  will be dependent on the monomer concentration. For varying  $[\text{TiCl}_4]$  concentrations,  $k_p'$  and  $k_p^\wedge \approx k_p''$  can be used to predict conversion data from eqs 2 and 3, respectively. This is especially important in block copolymer synthesis where reaching near 100% conversion of the IB charge prior to addition of the second monomer was shown to be essential for good blocking.<sup>8</sup> Equation 2 was used to simulate conversion–time and MWD–conversion plots using the Predici software package (CiT GmbH, Dr. M. Wulkow) and the agreement was found to be very good.<sup>28</sup> Detailed simulation studies using the comprehensive scheme with individual rate constants will be published elsewhere. We will only mention here that the S curve at a large excess of  $[\text{I}]_0$  over  $[\text{TiCl}_4]_0$ , shown in Figure 3, can be simulated by setting  $k_0 < k_1$ .

**Real-Time Conversion Monitoring of IB Polymerizations.** In the course of our kinetic studies we recognized a need for a convenient, real-time method of monitoring IB consumption. The first report of real-time monitoring of carbocationic polymerization of IB and styrene using a fiber optic ATR IR probe has been published.<sup>28</sup> The flexible fiber optic cable allows for easy maneuverability and the probe is immersed directly in the reaction vessel. This arrangement is more facile than the conduit technology reported recently.<sup>29</sup> In this report, the disappearance of the  $887 \text{ cm}^{-1}$  wag of the  $=\text{CH}_2$  group in IB was followed. The reported IR first-order plot was not linear, and the nonlinearity was explained by the exothermic nature of the reaction. It should be noted that the initial exotherm is more pronounced with aromatic initiators used in the ReactIR study, compared to TMPCl used in our studies. Another explanation given recently by the same authors<sup>30</sup> was that baseline shift due to concentration change upon monomer addition causes the nonlinearity at high conversion, and the problem can be solved with a correction factor. Figures 10 and 11 show two representative real-time IR plots recorded in our laboratory using high IB concentration (3 mol/L). Disappearance of the C=C double bond stretching at  $1656 \text{ cm}^{-1}$  and the C–H bending in the  $\text{CH}_3$  group of IB at  $1375 \text{ cm}^{-1}$  and the appearance of the doublet characteristic of the C–H bending in the *tert*-butyl groups of the forming PIB at 1365 and  $1390 \text{ cm}^{-1}$  were monitored. Conversions were calculated by assuming that concentrations (IB and PIB) were proportional to the corresponding peak heights. The agreement between IR and conventional (gravimetric) kinetic data, shown in Figure 12, is excellent in all four cases. It is evident that these peaks can be used for the convenient real-time monitoring of IB polymerization. With these peaks, solvent interference due to dilution is not a factor. It is also evident, however, that the first-order plots are not linear. The nonlinearity is most probably due to the polymerization exotherm, as suggested;<sup>30</sup> at lower IB concentration but otherwise identical conditions the first-order plot was found linear.<sup>28</sup> It should be mentioned here that higher polymerization exotherm is experienced when aromatic

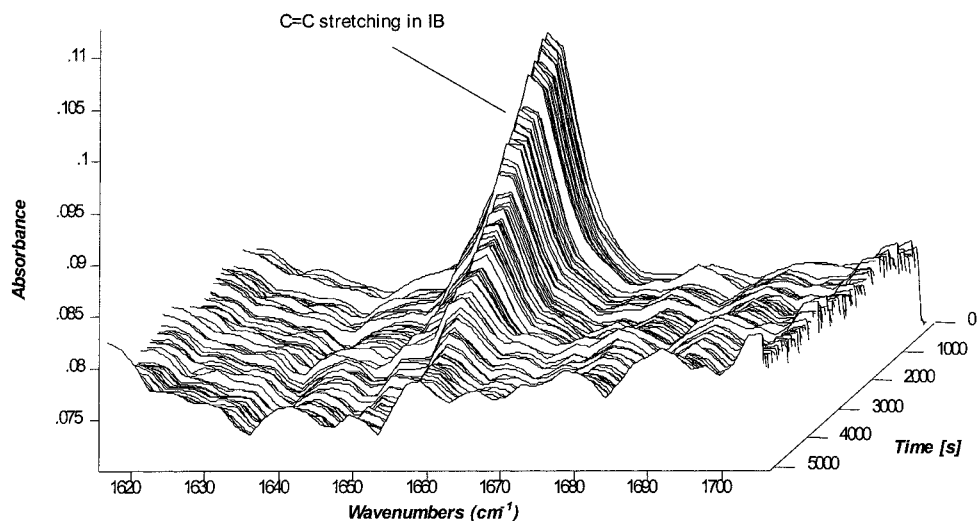


**Figure 10.** Real-time FTIR plot in IB polymerization at  $-80\text{ }^{\circ}\text{C}$ . C=C stretching of isobutene at  $1656\text{ cm}^{-1}$ ;  $[\text{TiCl}_4]_0 = 37 \times 10^{-3}\text{ M}$ ,  $[\text{IB}]_0 = 2.98\text{ M}$ ;  $[\text{DTBP}] = 7.0 \times 10^{-3}\text{ M}$ ;  $[\text{TMPCl}]_0 = 2.0 \times 10^{-3}\text{ M}$ ;  $\text{MeCHx/MeCl} = 60/40\text{ (v/v)}$ .

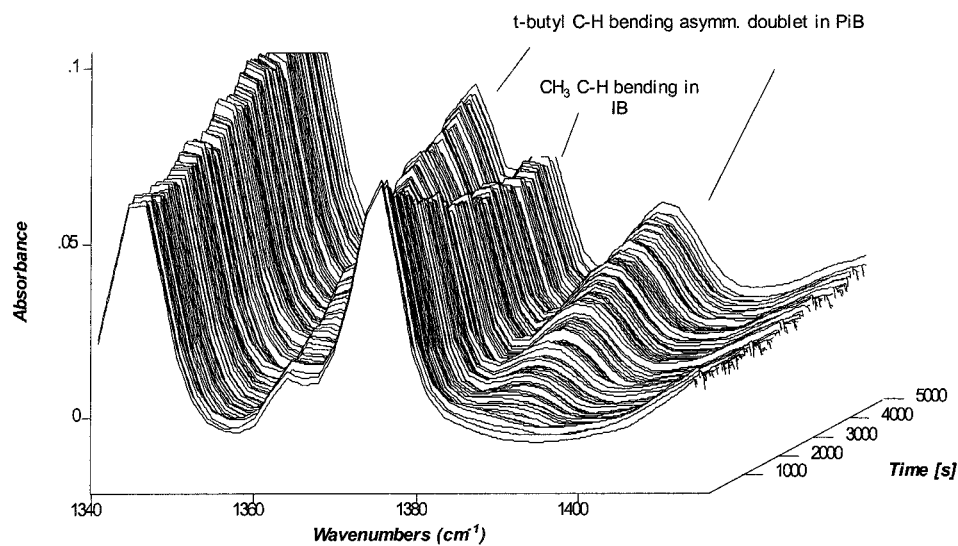


**Figure 11.** Real-time FTIR plot in IB polymerization at  $-80\text{ }^{\circ}\text{C}$ .  $[\text{TiCl}_4]_0 = 37 \times 10^{-3}\text{ M}$ ,  $[\text{IB}]_0 = 2.98\text{ M}$ ;  $[\text{DTBP}] = 7.0 \times 10^{-3}\text{ M}$ ;  $[\text{TMPCl}]_0 = 2.0 \times 10^{-3}\text{ M}$ ;  $\text{MeCHx/MeCl} = 60/40\text{ (v/v)}$ .

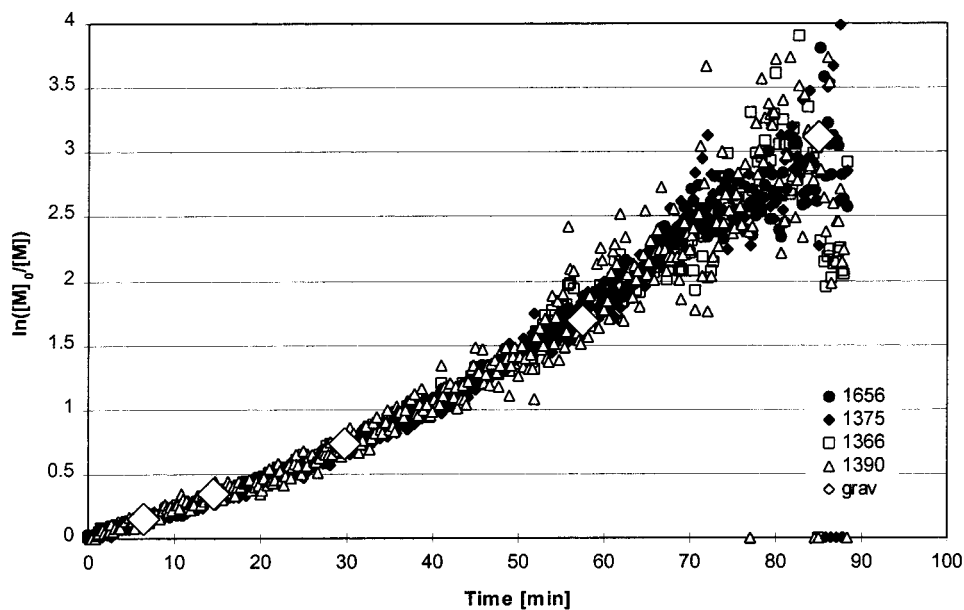


**Figure 12.**  $\ln([M]_0/[M])$  vs time plot for IB polymerization at  $-80\text{ }^{\circ}\text{C}$ : comparison between gravimetric and FTIR measurement;  $[\text{TiCl}_4]_0 = 37 \times 10^{-3}\text{ M}$ ,  $[\text{IB}]_0 = 2.98\text{ M}$ ;  $[\text{DTBP}] = 7.0 \times 10^{-3}\text{ M}$ ;  $[\text{TMPCl}]_0 = 2.0 \times 10^{-3}\text{ M}$ ;  $\text{MeCHx/MeCl} = 60/40\text{ (v/v)}$ .

initiators are used; hence the nonlinearity is observed at lower IB concentration.<sup>30</sup>

The fiber optic IR method demonstrated here is presently being further developed in our laboratory and will be used for future kinetic studies.

**Acknowledgment.** The authors would like to thank C. Paulo for repeating the Kaszas experiments, B. Brister for useful discussions and editing, Dr. P. Melling (Remspec) for consultation, and the Rubber Division of Bayer Inc., Canada, NSERC, and MMO (Materials and Manufacturing Ontario) for financial support.

## References and Notes

- (1) Gyor, M.; Wang, H. C.; Faust, R. *J. Macromol. Sci.* **1992**, A29, 639.
- (2) Storey, R. F.; Chisolm, B. J.; Mowbray, E. *Polym. Prepr.* **1993**, 34 (1), 568.
- (3) Fodor, Z.; Gyor, M.; Wang, H.-C.; Faust, R. *J. Macromol. Sci.* **1993**, A30, 349.
- (4) Kaszas, G.; Puskas, J. E. *Polym. React. Eng.* **1994**, 2 (3), 251.
- (5) Storey, R. F.; Chisolm, B. J.; Brister, L. B. *Macromolecules* **1995**, 28, 4055.
- (6) Storey, R. F.; Shoemaker, K. A. *Polym. Prepr.* **1995**, 36 (2), 304.
- (7) Storey, R. F.; Choate, K. R., Jr. *Macromolecules* **1997**, 30, 4799.
- (8) Storey, R. F.; Chisolm, B. J.; Lee, Y. *J. Macromol. Sci., Pure Appl. Chem.* **1994**, A31, 969.
- (9) Zsuga, M.; Kelen, T.; Balogh, L.; Majoros, I. *Polym. Bull.* **1992**, 29, 127.
- (10) Kelen, T.; Zsuga, M.; Balogh, L.; Majoros, I.; Deak, G. *Makromol. Chem., Macromol. Symp.* **1993**, 67, 325.
- (11) Kaszas, G.; Puskas, J. E.; Kennedy, J. P. *J. Macromol. Sci.* **1989**, A26, 1099.
- (12) Kaszas, G.; Puskas, J. E.; Kennedy, J. P. *J. Makromol. Chem., Macromol. Symp.* **1988**, 13/14, 473.
- (13) Zsuga, M.; Kennedy, J. P. *Polym. Bull.* **1989**, 21, 5.
- (14) Roth, M.; Patz, M.; Freter, H.; Mayr, H. *Macromolecules* **1997**, 30, 722.
- (15) Kennedy, J. P.; Majoros, I.; Nagy, A. *Adv. Polym. Sci.* **1994**, 112, 1.
- (16) Puskas, J. E.; Kaszas, G.; Litt, M. *Macromolecules* **1991**, 24, 5278.
- (17) Rytter, E.; Kvisle, S. *Inorg. Chem.* **1985**, 24, 640.
- (18) Griffiths, J. E. *J. Chem. Phys.* **1968**, 49, 642.
- (19) Hadjikyriacou, S.; Faust, R. *Macromolecules* **1995**, 28, 7893.
- (20) Moreau, M. IP '97 (International Symposium on Ionic Polymerizations and Related Processes) Proceedings, Paris, 1997; p 135.
- (21) Kaszas, G.; Gyor, M.; Kennedy, J. P.; Tudos, F. *J. Macromol. Sci., Chem.* **1982/83**, A18, 1367.
- (22) Puskas, J. E.; Hutchinson, R. *Rubber Chem. Technol.* **1994**, 66 (5), 746.
- (23) Kaszas, G.; Puskas, J. E.; Kennedy, J. P.; Hager, W. G. *J. Polym. Sci.* **1991**, A29, 427.
- (24) Roth, M.; Mayr, H. *Macromolecules* **1996**, 29, 6104.
- (25) Kamigaito, M.; Yamaoka, K.; Sawamoto, M.; Higashimura, T. *Macromolecules* **1992**, 25, 6400.
- (26) Creaser, C. S.; Creighton, J. A. *J. Chem. Soc., Dalton Trans.* **1975**, 1402.
- (27) Kistenmacher, T. J.; Stucky, G. D. *Inorg. Chem.* **1970**, 10, 122.
- (28) Puskas, J. E.; Lanzendörfer, M. G.; Pattern, W. E. *Polym. Bull.* **1998**, 40, 55.
- (29) Storey, R. F.; Donnalley, A. B.; Maggio, T. L. *Macromolecules* **1998**, 31, 1523.
- (30) Storey, R. F.; Donnalley, A. B.; Maggio, T. L. Private communication, 1998.

MA980934W